JPE 6-4-5

Modeling of a Switched Reluctance Motor in Sensorless and "With Sensor" Modes

G. Bhuvaneswari†, Sarit Guha Thakurta*, P. Srinivasa Rao* and S. S. Murthy*

†*Dept. of Electrical Engg., Indian Institute of Technology, Delhi, India

ABSTRACT

Switched Reluctance Motors (SRM) have emerged as viable alternatives to other adjustable speed drives such as vector controlled induction motors (VCIM) and permanent magnet brush-less (PMBL) motors due to their simple construction, ease of control, low inertia and higher operating speeds. However, the indispensability of the rotor position sensor in an SRM for its successful operation increases its cost, apart from causing other problems like decreasing its reliability and inability to operate in adverse environmental conditions. In this paper, a new sensorless control scheme for the SRM is advocated. The required fundamental data is obtained by analyzing the SRM using the Finite Elements (FE) package MAXWELL. The drive is studied in both "with sensor" and "sensorless" modes and a comparison of the performances, in both cases, is presented for various operating conditions.

Keywords: Switched Reluctance Motor, rotor position sensor, sensorless control

1. Introduction

The variable speed drive market is seeing a change with Switched Reluctance Motor (SRM) drives effectively competing with conventionally used induction motors. This is mainly due to the simple, rugged, reliable and inexpensive structure of SRMs coupled with their high torque-to-inertia ratio. A high starting torque without a high inrush current and a power density comparable to conventional induction motors make the SRM a very promising motor for the future. Though there are several features in favor of SRMs, they have not gained enough popularity due to the complexities of the control involved. The closed loop control of an SRM drive is implemented using a power electronic converter [1] and is achieved by sensing the phase current, absolute rotor position and rotor speed. Rotor position sensing is an integral part of SRM control because of the nature of the reluctance torque production. In fact, excitation of the SRM phases needs to be properly synchronized with the rotor position for effective control of speed, torque and torque pulsations [2-4]. A shaft position transducer is usually employed to determine the rotor position. Any form of rotor position sensor adds complexity and cost to the system. Moreover, electromagnetic interference and temperature effects tend to reduce the reliability of the position sensing system. In order to avoid these difficulties, some form of indirect position sensing scheme is desirable.

Various forms of sensorless control techniques have been presented in the literature [5-7]. In [8], a review of sensorless control techniques has been presented and the existing techniques have been classified under hardware intensive,

Manuscript received June 15, 2006; revised August 16, 2006
†Corresponding Author: bhuvan@ee.iitd.ernet.in
Tel: +91-11-2659-1092, Fax: +91-11-2658-1606, IIT. Delhi
*Dept. of Electrical Eng., Indian Institute of Technology, Delhi, India

data intensive and speed intensive schemes. The methodology that is being used in this paper falls under the category of data intensive sensorless technique. Fahimi and others discuss an adaptive fuzzy-logic based sensorless control technique in [9] that is suitable for a wide range of speeds in an SRM drive. In the present work, Finite Element (FE) analysis of the SRM has been carried out using the FE package Maxwell SV [10] to obtain magnetization characteristics. The magnetization characteristics obtained have been utilized to deduce the rotor position given the operating voltage and current of the phase winding. The performance of the SR motor has been analyzed and compared in both "with sensor" and "sensorless" modes. The analysis has been carried out in Simulink/MATLAB environment [11]. The methodology adopted for the analysis of the SRM drive system, the results obtained from the analysis during starting, load perturbation and reference speed variation have been presented for both cases and conclusions thus drawn are presented in the following sections.

2. Methodology

To simulate the control of SRM in the "sensor" mode, a linear inductance profile has been assumed for the stator winding of the SRM. When the motor is operated as a stepper motor, the step angle is given by

$$\theta_s = 2\pi\left(\frac{1}{N_r} - \frac{1}{N_s}\right) \tag{1}$$

where N_r and N_s are the number of rotor and stator poles, respectively. The voltage equation for each phase is given by,

$$V = i_j R + \frac{d\psi(\theta, i_j)}{dt} \tag{2}$$

where V is the applied voltage, i_j is the current through the jth phase winding, R is the resistance of the phase winding and ψ is the flux linkage at rotor position θ. While ignoring the effect of saturation, the flux in each phase is given by the linear equation

$$\psi_i(\theta, I_i) = L(\theta) I_i \tag{3}$$

The torque generated by each stator phase is

$$T_{ph} = 0.5\, i_j^2 \{dL(\theta, i_j)/d\theta\} \tag{4}$$

The total electromagnetic torque T_e is the addition of the torques developed by each of the phases in the stator. The mechanical equation is

$$J\frac{d\omega}{dt} = T_e - T_l \tag{5}$$

where T_l represents the load torque, J is the moment of inertia of the drive system and ω is the angular velocity of the rotor. The above equations are translated into a model as shown in Fig. 1 and implemented in SIMULINK/ MATLAB environment. The motor considered in the present work has 8 stator poles (4 phases) and 6 rotor poles where the consecutive stator phases are displaced from each other by 45°. Each of the stator phases is represented by a block named 'Phase n' where 'n' stands for the stator phase number. The turn-on angle (θ_{ON}) of the device in the power electronic converter which energizes any particular phase, is also one of the input to this block.

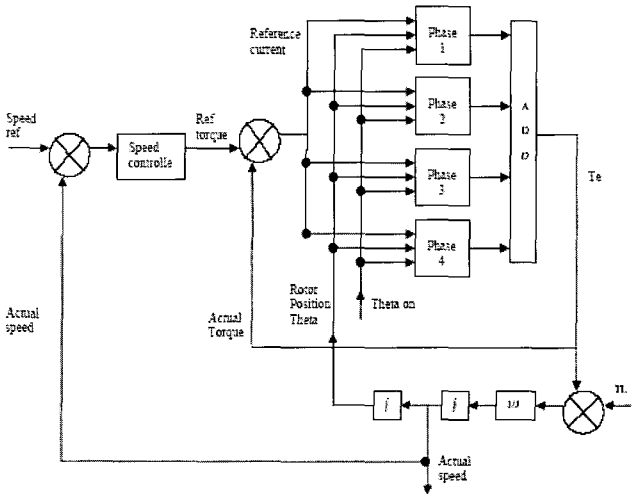

Fig. 1 Block diagram of the SRM drive with position sensor

2.1 Simulation of SRM with Sensor

Fig. 2 shows the contents of the block *'Phase 1'* in simulation of SRM with a rotor position sensor. It consists of four blocks, each one associated with a specific MATLAB function. They are the following:

- *Period* – Each phase inductance has a periodicity of $2\pi/N_r$ degrees. Therefore, it is appropriate to transform the rotor position θ obtained from the mechanical equation as a modulus of $2\pi/N_r$. In Fig. 2, the block *period* achieves this function.

- *Commutation* – This block ensures the conduction and commutations of the power devices in the mid point H-bridge converter [1-2] at appropriate time instants with respect to rotor position θ. The hysteresis current controller ensures that the current is maintained at the required value. The angle at which a particular phase is energised, i.e., θ_{ON} is also one of the input to this block.

- *Inductance* – This block computes the current through the particular phase winding based on its inductance, resistance and the applied voltage. The inductance value depends on rotor position θ.

- *Torque* – This block computes the torque produced by this particular phase. The two input to this block are the current obtained from the previous block and dL/dθ.

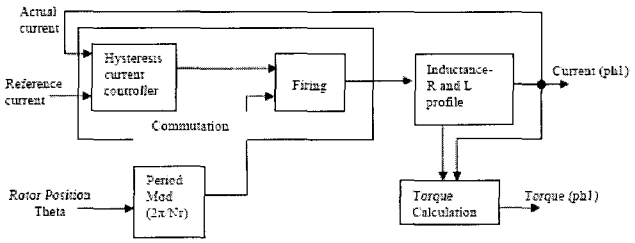

Fig. 2 Model for Phase 1 in Simulation "with sensor"

2.2 Simulation of SRM in Sensorless mode

As mentioned earlier, the sensorless control technique used in the present work is a data intensive technique. The data corresponding to the magnetization characteristics of the SRM has been obtained from the magnetic analysis of the motor. The air gap flux is a function of rotor position θ and the current through the phase winding 'i'. The magnetic analysis of the machine has been carried out in 'Maxwell SV' [10] to obtain the flux plots of the machine for different values of phase currents within the operating range (i.e., 0 to 18 Amp) and for various rotor positions. The dimensions of the machine (as in Table 1 obtained from the manufacturer of the SRM- TASC drive, UK) have been provided as software input data. The corresponding flux and torque values have been obtained as shown in Fig.3. Thus, flux-current-θ (ψ-i-θ) and torque-current-θ (T-i-θ) look-up tables have been formulated for the SRM.

In the Simulink model of the SRM in sensor-less mode, these look-up-tables have been utilized to deduce the rotor position. The flux is calculated as the integral of the applied voltage less the resistance drop during the sampling interval. The ψ-i-θ look-up table is used to estimate the rotor position, for a given value of current and flux, which in turn is used to determine the torque from the T-i-θ look-up table. The updated value of current is recalculated using the new value of flux. Fig. 4 shows the schematic diagram of the Simulink/MATLAB model for sensorless control of the SRM. The current control is achieved using a hysteresis current controller.

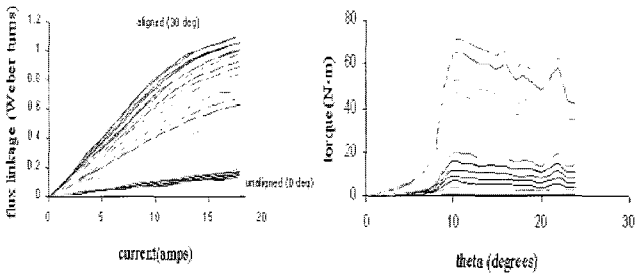

Fig. 3 Flux linkage-current-Theta and Torque-current-theta characteristics

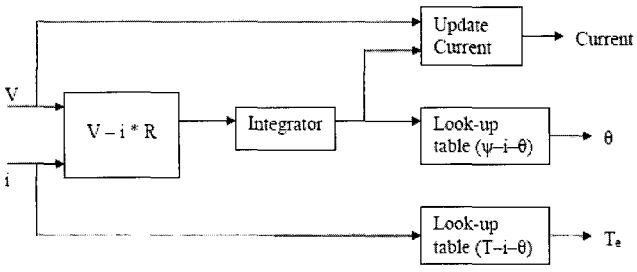

Fig. 4 Model for 'Phase 1' in sensor-less mode

3. Results

The models that have been presented so far are used to estimate the performance of the SRM drive for different

operating conditions in both "with sensor" and "sensorless" modes. The results obtained are presented in the following sections.

Table 1 Dimensions of SRM used for FE Analysis in Maxwell

Stator		Rotor	
Winding	4 phase, 8/6 pole	Rotor Material	Silicon sheet steel
Core material	silicon sheet steel	Rotor pole tip diameter	95.5162 mm
Stator bore diameter	96.2162 mm	Rotor pole arc	21 degrees
Stator core outer diameter	160 mm	Shaft diameter	44.7 mm
Stator back iron width	10 mm	Air gap width	0.35 mm
Stator pole arc	21 degrees	Stack depth	150 mm
		Rotor pole height	16 mm
Stator coil dimensions			
Conductor size	1.8618 mm (diameter for circular conductors)		

When the SRM drive is simulated with a position sensor, a linear magnetic circuit has been assumed with ($dL/d\theta$) being a constant. Fig. 5 shows the inductance profile of phase 1 which varies linearly between L_{max} (120 mH) and L_{min} (10mH). Each phase is staggered from the adjacent phase by 45°. The phase current and phase torque, in steady state, during no load for both sensor and sensor-less cases are shown in Fig. 6 (a) and (b) respectively. Initially the inductance is at the minimum value, resulting in a very small value of induced emf and hence a rapid rise in the current. Then, the hysteresis current controller ensures the current is limited to the maximum value of 4 A (in sensor case) by current chopping that is sufficient to meet the frictional torque requirement at no-load condition. In the sensor-less case, the current is found to be much less but the torque profile has improved due to the fact that saturation plays a vital role in increasing the co-energy.

The torque and speed responses during starting and load disturbance are shown in Fig. 7 for both sensor and sensor-less cases. It can be seen from Fig. 7 (a) that the speed rise is almost linear with a rise time of about 0.04 sec with hardly any overshoot, while the drive is operating with a position sensor. The motor is able to reach its reference speed within 0.025 sec in the sensor-less case. The peak starting current is set at about 28 A which is within the maximum current carrying capability of the phase winding (i.e., 30 A). At t=0.25 sec, a load torque of 24 Nm is applied to the motor shaft while the full-load torque capability of the motor is about 27 Nm. The rotor experiences a dip of 3 rad/sec in speed and the electromagnetic torque developed by the motor quickly jumps to 24 Nm. The speed regulation is less than 4% throughout the operating range. In the sensor-less case, as shown in Fig. 7 (b), the rotor experiences a speed dip of 2 rad/sec while applying load, which corresponds to a speed regulation of 1.27%. At t=0.35 sec, the load is thrown off resulting in a torque demand of 2 Nm. This results in a slight rise in speed in both the sensor and sensor-less cases Subsequently, the motor attains the original steady state speed of 157 rad/sec. The dip in speed during load disturbance is much less in the sensor-less case as compared to the sensor case. This is essentially due to the fact that the sensorless case takes into account magnetic saturation while the "with sensor" case does not. The currents drawn by phases 1 and 2 during load disturbance are shown in Fig. 8 for both sensor and sensor-less modes. It is clearly seen that in "with sensor" mode the machine draws a much larger current than the "sensorless" mode for developing the same amount of electro-magnetic torque due to the constant ($dL/d\theta$) being assumed in the former case.

The response of SRM as a variable speed drive is shown in Fig. 9. The reference speeds are set at 50, 100 and 157 radians /sec at 0, 0.1 and 0.15 sec respectively. It is observed that the actual speed of the motor closely follows the reference speed although there is an overshoot in speed close to 57 rad/sec at t=0.02 sec. Whenever there is change in the reference speed, the current drawn increases to meet the accelerating torque demand. The response of the SRM to reference speed variation, in sensorless mode is shown in Fig. 9(b), which is also satisfactory.

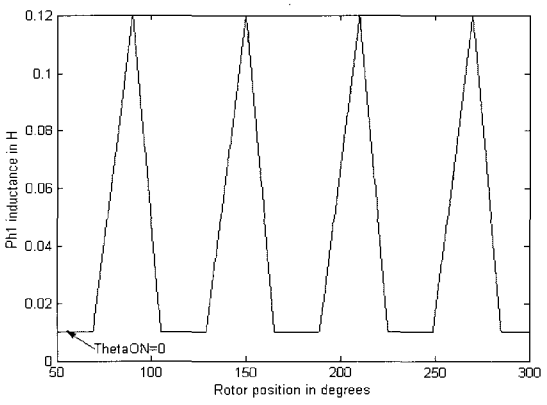

Fig. 5 Inductance variation in phase 1 with rotor position

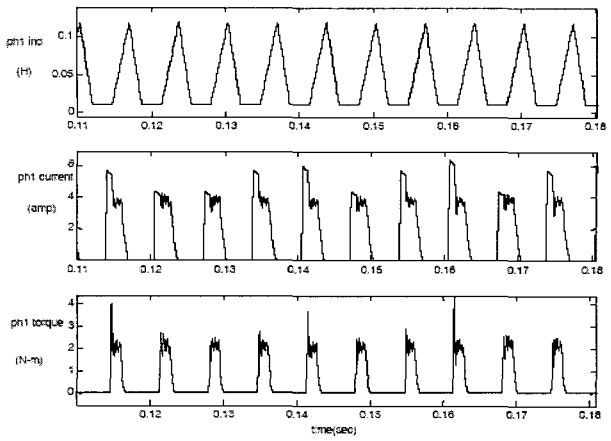

Fig. 6(a) Variation in phase current and torque during no load in sensor mode

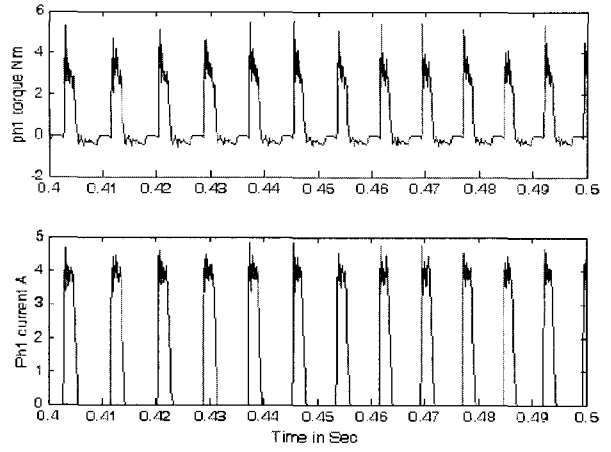

Fig. 6(b) Variation in phase current and torque during no load in sensorless mode

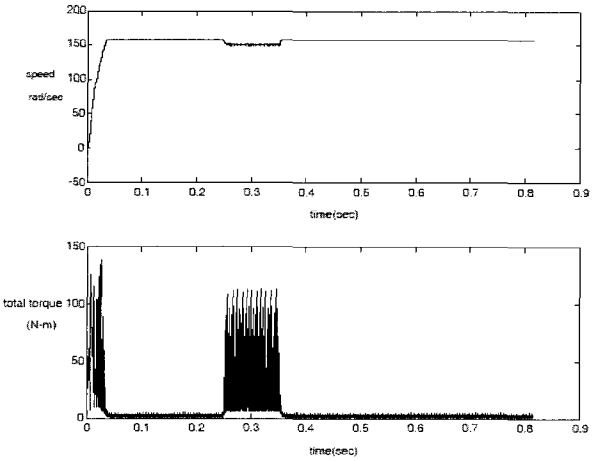

Fig.7(a) Speed and total torque during load disturbance in "sensor" mode

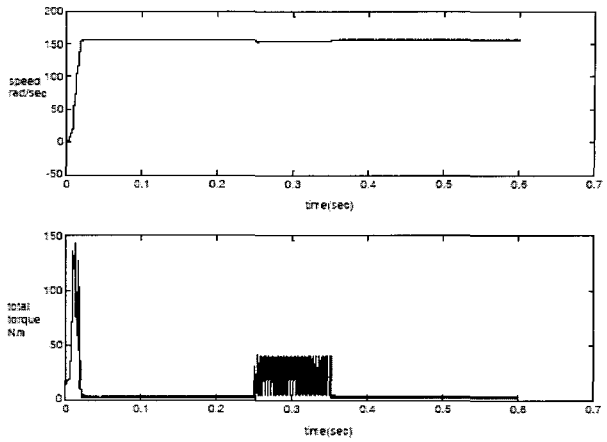

Fig.7(b) Response of the SRM in sensor-less mode during starting and load disturbance

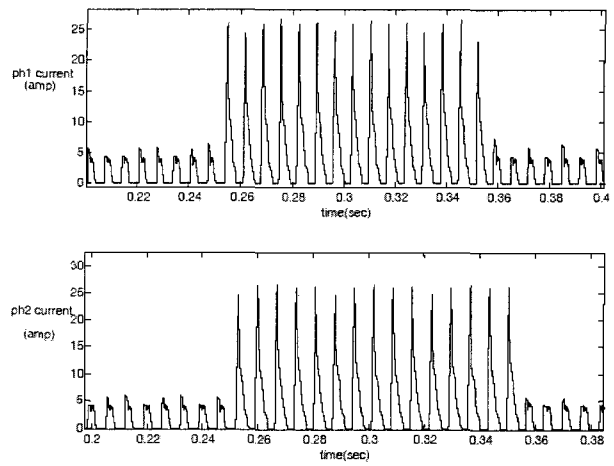

Fig. 8(a) Current profiles of phases1 and 2 during load disturbance in "sensor" mode

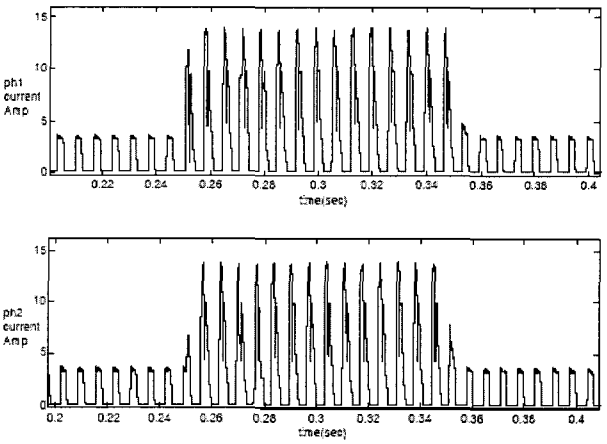

Fig. 8(b) Current profiles of phases 1 and 2 during load disturbance in sensorless mode

4. Comparison of performance of SRM with and without sensors

The comparative study of the results obtained in "with sensor" and sensorless control schemes of the SRM drive is presented in this section. In the case of the SRM "with sensor", a linear inductance profile has been assumed. The rate of inductance variation, with respect to the rotor position, is assumed to be a constant which is not the case when the magnetic circuit is in the saturation region. In the sensorless case, it should be expected that the torque production and the response in general should be better than the "with sensor" case, where the inductance varies linearly resulting in equal amounts of energy and co-energy in the magnetization characteristics. This is very clearly seen in the starting response of the SRM. In the control scheme of the SRM with sensor, the rise time of the speed response curve is 0.04 sec whereas in the sensorless scheme it is observed to be 0.025 sec. In the linear case, the energy and co-energy portions of the ψ-i characteristics would be exactly equal to each other. As the rate of change of co-energy is the electromagnetic torque, obviously, it is less in the linear case as compared to the non-linear case where the co-energy is more than the field energy. This enhances torque production in the sensor-less case, for the same amount of input electrical energy, thus improving the response of the drive.

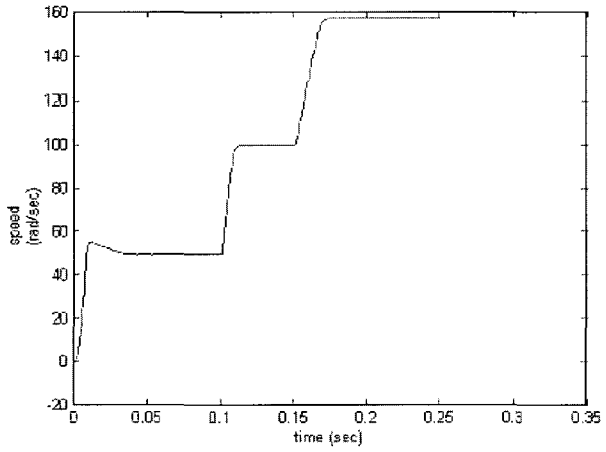

Fig. 9(a) Response of SRM in sensor mode for different reference speed settings

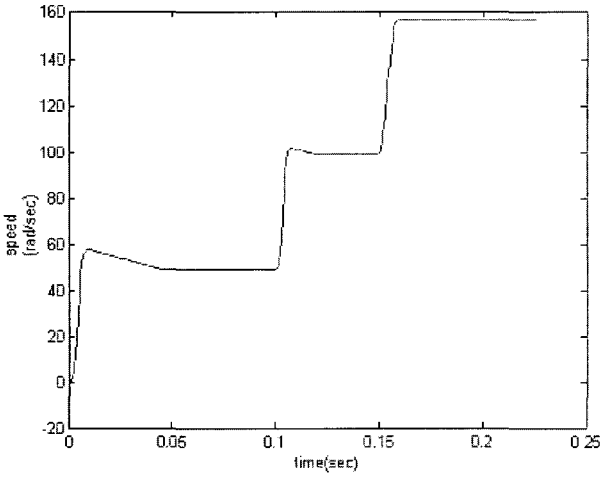

Fig. 9(b) Variable speed response in sensorless mode

During the load disturbance it is observed that while controlling the drive "with sensor", the peak current drawn by the motor is almost 22 A, whereas in the sensor-less control scheme it is 15 A. The current is effectively limited by the enhanced value of back emf due to the non-linear profile of the inductance of the machine in the sensorless mode. Looking at the response of the drive in various operating conditions in "with sensor" and sensorless mode, it can be said that the sensorless control gives a better response under most of the operating conditions.

However, the major drawback of the sensorless technique adopted here is it is not adaptive [8]. Hence, it will not take into account the parameter variations of the drive for various ranges of operating speed and torque. In some of the speed-intensive techniques [9], on-line predictive control schemes are adopted that can adapt according to the operating speed of the drive. But, these control schemes will prove to be complex.

5. Conclusions

This paper has presented modeling and analysis of a SRM under various operating conditions in sensorless and "with sensor" modes. A novel method of sensorless control of the SRM has been advocated using the magnetization characteristics of the motor obtained from the FE package MAXWELL SV. The performance of the motor has been studied using the simulation package Simulink/MATLAB environment with and without

position sensors. The simulation results obtained in both schemes have been presented and discussed thoroughly for different operating conditions like starting, load disturbance and variation in the reference speed. Finally, a comparison is made between the responses obtained from both the schemes. It can be said that sensorless control schemes are more reliable and suitable for the SRM drive if it is to be operated over a specific speed range for which the parameters of the SRM drive remain fairly constant.

References

[1] A. K. Jain and N. Mohan, "SRM power converter for operation with high demagnetization voltage", IAS annual meeting 2004. pp 1625-1631.

[2] T. J. E. Miller, Switched Reluctance Motors and their Control, *Oxford University Press and Magna Physics Publications,* ISBN 0-19-859387-2 (UK); 9 780198593874 (USA), 1993.

[3] T. J. E. Miller (ed.), Electronic Control of Switched Reluctance Machines, *Newnes Power Engineering Series*, ISBN 0 7506 50737 (UK), 2001.

[4] R. Krishnan, Switched Reluctance Motor Drives: Modelling, Simulation, Analysis, Design, and Applications, *Industrial electronics Series, CRC Press*; 2001.

[5] Mehrdad Ehsani and B. Fahimi, "Elimination of Position Sensors in Switched Reluctance Motor Drives: State of the Art and Future Trends", *IEEE Transactions on IE, Vol. 49*, No. 1, pp. 40 – 47, 2002.

[6] Fedigan, J. Stephen, Cole, P. Charles, "A variable speed sensorless drive system for Switched Reluctance Motors", *Texas Instruments Application Report* SPRA, October '99.

[7] N. Inanc and V. Ozbulua, "Torque Ripple minimization of a switched reluctance motor by using continuous sliding mode control technique", *Electric Power Systems Research 66* (2003) pp 241-251.

[8] B. Fahimi, A. Emadi and R. B. Sepe Jr., "Position Sensorless Control", IEEE IA magazine, Jan-Feb 2004 pp.40-47.

[9] B. Fahimi, A. Emadi and R. B. Sepe Jr., "Four Quadrant position sensorless control of SRM drives over the entire speed range", IEEE Transactions on PE, Jan 2005 pp. 154-163.

[10] Maxwell SV and its online documentation www.ansoft.com/maxwellsv

[11] Matlab 6.1 with Simulink & associated manuals www.mathworks.com

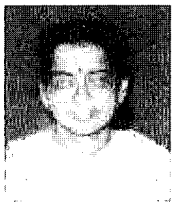

G. Bhuvaneswari obtained her Masters and Doctoral degrees from the Indian Institute of Technology, Madras, India. She has been with the Department of Electrical Engineering. IIT, Delhi since 1997 as a faculty member. She is a senior member of IEEE, USA. Her areas of interest are power electronics, machines, drives and power quality.

Sarit Guha Thakurta obtained his B. Tech. degree from IIT Delhi, India and M. S. from ETH, Zurich, Switzerland. He is currently working with Cypress Semiconductors as an IC designer.

P. Srinivasa Rao obtained his Masters' degree from the Department of Electrical Engineering, IIT, Delhi in 2003. He is currently working with Patni Computers in the area of Embedded System Design.

S. S. Murthy is with the Department of Electrical Engineering, IIT, Delhi as a professor. He is a fellow of IEE, UK and a senior member of IEEE. He was the director of NIT, Surathkal for a period of 2 years. His areas of interest are induction generators, power electronics and electric drives.